Andreev spectrum with high spin-orbit interactions: revealing spin splitting and topologically protected crossings.

A. Murani[1], A. Chepelianskii[1], S. Guéron and H.Bouchiat[1]
[1] *1Laboratoire de Physique des Solides, CNRS, Univ. Paris-Sud, Université Paris Saclay, 91405 Orsay Cedex, France*

We investigate numerically the Andreev spectrum of a multichannel mesoscopic quantum wire (N) with high spin-orbit interaction coupled to superconducting electrodes (S), contrasting topological and non topological behaviors.In the non topological case, modeled by a square lattice with Rashba interactions, we find that as soon as the normal quantum wires can host several conduction channels, the spin degeneracy of Andreev levels is lifted by a phase difference between the S reservoirs which breaks time reversal symmetry in zero Zeeman field. The Andreev states remain degenerate at phases multiple of π for which time reversal symmetry is preserved, giving rise to level crossings which are not lifted by disorder. In contrast with the dc Josephson current, the finite frequency admittance (susceptibility) is very sensitive to these level crossings and the lifting of their degeneracy by a small Zeeman field. More interesting is the case of the hexagonal lattice with next nearest neighbor spin-orbit interactions which exhibit 1D topological helical edge states [1]. The finite frequency admittance carries then a very specific signature at low temperature of a protected Andreev level crossing at π and zero energy in the form of a sharp peak split by a Zeeman field.

PACS numbers:

INTRODUCTION

A number of intriguing phenomena have been predicted recently when quantum wires made from materials with strong spin-orbit interaction (SO) are used as weak-links coupling two superconductors : Spin-dependent supercurrents [2–4] supercurrents through edge-states when the wire is made of a topological insulator [1, 5] supercurrents at zero phase difference (ϕ_0 junctions) [7–10], topologically protected zero-energy states [5, 6]. Different materials have been used to explore experimentally some of these ideas: semiconducting nanowires (InAs or InSb), demonstrating ϕ_0 junctions [12] and probing Majorana physics [13–17], and HgTe/HgCdTe or InAs/GaSb quantum wells heterostructures [18, 19], BiSe flakes[20], Bi nanowires [21, 22] revealing supercurrent through helical edge states.

Spin-orbit interaction, by coupling the kinetic momentum to the electronic spin, is known to break the spin degeneracy of electronic states in a quantum dot in the absence of any magnetic field. We consider here both the effect of the intrinsic atomic spin-orbit interaction specific of heavy atoms and are at the origin of the emergence of the spin-Hall insulator state for the hexagonal 2D lattice [1, 11] and the Rashba [23] spin-orbit interaction $H_R \propto \vec{E}_R.(\vec{p} \times \vec{\sigma})$ at 2D interfaces of semiconductors where inversion symmetry is broken by a perpendicular electric field $\vec{E}_R$. In the case of a purely 1D wire along the x axis the Rashba spin-orbit coupling [23], $H_{R\|} = \lambda_R p_x \sigma_y$ commutes with the 1D kinetic momentum. The spin components of the eigen states are polarized along or opposite to the y axis. Their spatial components are Bloch waves whose wave vector are shifted by $\pm k_{SO} = 2m_{eff}\lambda_R/\hbar^2$ depending on the spin direction. When the wire has a finite width allowing the formation of several transverse channels with different k_y, the transverse component of the Rashba Hamiltonian $H_{R\perp} = \lambda_R p_y \sigma_x$ couples the longitudinal components of the wave functions corresponding to different channels. The eigen-states which energy is close to the crossing points between these different channels acquire different velocities along the x axis as shown on Fig.1 They are not uniformly spin polarized but display a spatially dependent spin texture [24].

When the quantum wire is strongly coupled to superconducting reservoirs, proximity induced superconductivity leads to the formation of Andreev pairs which are the combination of time reversed electron and hole states. Time reversal symmetry imposes that these Andreev states keep their spin degeneracy in the presence of SO interaction. This is however no longer the case when the two superconducting reservoirs impose a finite phase difference ϕ on the boundary conditions of Andreev states. When this phase factor is different from an integer multiple of π, Andreev wave functions acquire imaginary components and Andreev levels loose their two-fold degeneracy. The phase dependence of Andreev levels is therefore split in the presence of SO interaction. This is the signature of a spin supercurrent which coexists with the charge supercurrent when time reversal symmetry is broken.

In the second section of this paper we first investigate the conditions to induce spin split Andreev states in the absence of any Zeeman field in a non topological wire. This is illustrated by numerical results obtained by diagonalizing the Bogolubov Hamiltonian of a quantum wire with a square lattice and Rashba spin-orbit interaction between superconducting electrodes. The effects of the

geometry of the junction (length, number of channels), disorder, position of Fermi energy are discussed. The broken degeneracy of Andreev states at phases between 0 and π, is observed in the Andreev spectrum of multichannel wires as a result of the combination of electron and hole wave functions originating from different transverse channels k_y coupled through the transverse Rashba term $H_{R\perp} = p_y\sigma_x$. Whereas this effect is not significant in very short junctions of a few atomic sites [9] it strongly modifies the Andreev spectrum of long junctions even with disorder. We then discuss the Andreev spectrum of the 2D hexagonal lattice with next nearest neighbor spin-orbit couplings (equivalent to the implementation of atomic spin-orbit coupling at low energy) leading to a 2D topological insulator and a Quantum spin Hall state (Kane and Mele model [1]). As expected, we confirm for wide enough samples, the presence of 1D ballistic Andreev edge states crossing each other at zero energy and robust against disorder.

In section 3 we show that the Josephson current for non topological junctions is only weakly affected by SO interaction, with a decrease of the Josephson current in the absence of disorder but a substantial increase in the diffusive regime which can be understood as a signature of antilocalisation in the Andreev spectrum. On the other hand the phase dependence of the Josephson current exhibits a saw tooth shape, characteristic of 1D ballistic transport, for the hexagonal lattice in the topological quantum spin Hall state. This signature of 1D ballistic edge states does not however reveal the topological character of these states.

In contrast, we show in Section 4 that the non adiabatic linear response of the Josephson current to a high frequency phase modulation is extremely sensitive to level crossings or anticrossings in the Andreev spectrum at all energies below the superconducting gap. The dissipative response $\chi'' = i\omega Y$ has a contribution that is proportional to the sum of i_n^2, the square of the single level currents, in an energy window whose width is determined by temperature. A very small Zeeman field breaks the level degeneracy at 0 and π, yielding discontinuities in these single level currents and consequently sharp dips in χ''. The topological case is characterized by protected level crossings at zero energy and can be clearly identified in experiments measuring this dissipative response at very low temperature. χ'' exhibits a sharp peak at π which does not exist in the non topological case, and is split by a Zeeman field.

ANDREEV SPECTRUM WITH SPIN-ORBIT INTERACTION

Square lattice with Rashba spin-orbit interaction

We first consider the case of a wire described by a tight binding model on a 2D square lattice. We implement the Bogoliubov-de Gennes Hamiltonian described by the 4 blocks matrix:

$$\mathcal{H} = \begin{pmatrix} H - E_F & \mathbf{\Delta} \\ \mathbf{\Delta}^\dagger & E_F - H^* \end{pmatrix} \tag{1}$$

The BCS matrix $\mathbf{\Delta}$ couples electron and hole states of opposite spin, exclusively in the S part, and imposes the phase difference ϕ between the 2 superconducting reservoirs:

$$\mathbf{\Delta} = \mathbf{\Delta_{is,i's'}} = \exp(i\phi/2) \begin{pmatrix} 0 & -1 \\ 1 & 0 \end{pmatrix} \tag{2}$$

H and $-H^*$ are $N \times N$ matrices that describe respectively the electron- and hole-like spin dependent wave functions of the hybrid NS wire with Rashba spin-orbit interaction[23].

$$H = \sum_{s,s'=+,-} \sum_{i=1}^{N} \epsilon_i(|i,s><i,s| + |i,s'><i,s'|) + \sum_{i\neq j} t_{ij}|i,s><j,s| + i\lambda_{ij}(\vec{e_z} \times \vec{u_{ij}})\tilde{\sigma}|i,s><j,s'| + C.C. \tag{3}$$

The vector $\vec{u_{ij}}$ connects the nearest neighbor sites i and j , $\vec{e_z}$ is the unitary vector perpendicular to the plane of the sample, $\tilde{\sigma}$ is the vector of Pauli matrices $\sigma_{x,y,z}$. The wire has $\mathrm{N} = N^N + N^S = N_x \times N_y$ sites on a square lattice of period a, with a normal part of $N^N = N_x^N \times N_y$ sites in contact on both sides with superconducting regions of length $N_x^S/2$. ($N^S = N_x^S \times N_y$ sites). The on-site random energies ϵ_i of zero average and variance W^2 describe the disorder in the wire. The hopping and spin dependent coupling matrix elements $t_{ij} = t$ and $\lambda_{ij} = \lambda$ are restricted to nearest neighbors.

We have chosen the amplitude of the superconducting gap $\Delta = t/4$ and the number of superconducting sites larger than 30 such that the S coherence length $\xi_s = 2ta/\Delta \ll N_x^S$ in order to avoid any reduction of the superconducting correlations in the S region (inverse proximity effect). We have checked that increasing the number of S sites does not change the spectrum of Andreev states below the superconducting gap. The number of transverse channels and the amplitude of the disorder correspond to the diffusive regime where the length $L = N_x^N a$ of the normal region is longer than the elastic mean free path l_e and shorter than the localization length $N_y l_e$. The length l_e is related to the amplitude of disorder by $l_e \simeq 15a(t/W)^2$ at 2D [25]. In the following we will mostly focus on the long junction limit where $L \gg \xi_s$.

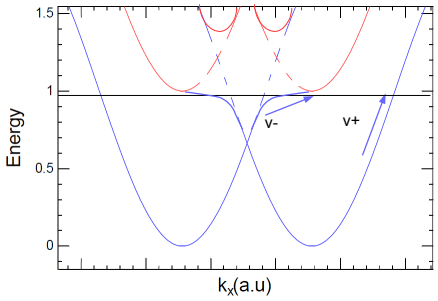

FIG. 1: Schematic tight binding band structure of a 2 channel ballistic wire in the presence of both longitudinal $H_{R\|}$ and $H_{R\perp}$ transverse Rashba spin-orbit interactions. The transverse Rashba coupling between the 2 channels $H_{R\perp}$ opens a gap at the 2 band crossings leading to a non parabolic asymmetric band structure with different velocities v^+, v^- when the Fermi energy lies just below this gap.

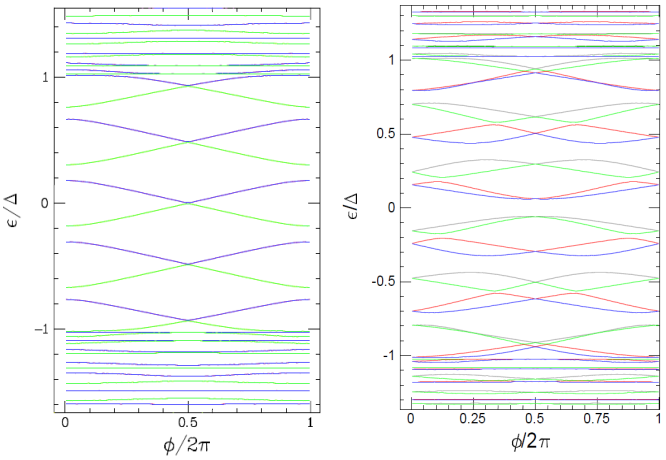

FIG. 2: Phase dependent spectrum of Andreev levels for 1D quasi ballistic wires ($L \ll l_e$)with one and two transverse sites in the long junction limit $N_x = 50$.Left: $N_y = 1$, $\lambda = 3\Delta$, the spectrum is the same as for $\lambda = 0$. Right: $N_y = 2$, $\lambda = 3$(The number of S sites are respectively $N^S = 100 \times 1$ and $N^S = 100 \times 2$). The Fermi energy is taken at 1/4 of the tight binding lower 1D band ($\epsilon_F = -t/2 = -2\Delta$) which corresponds to the bottom of the upper band, see Fig.2. Note the breaking of spin degeneracy for $N_y = 2$ which is absent in for $N_y = 1$ where the Andreev levels are spin degenerate.

We first consider a single channel 1D wire with $N_y = 1$. The Andreev spectrum shown in Fig.2 (right) contains 10 levels in the superconducting gap with avoided crossings at zero and π due to a small on site disorder. This Andreev spectrum remains spin degenerate in the presence of spin- orbit interaction. This can be simply understood considering that in this 1D limit, the effect of SO interaction can be cast into a phase shift which is opposite for electrons and holes and leaves the Andreev levels unchanged whatever the position of the Fermi energy.

The situation is very different when there are more than one transverse sites($N_y \geq 2$). A degeneracy breaking of the Andreev states shows up, due to the mixing between different transverse channels k_y coupled by $H_{R\perp} = p_y\sigma_x$. As a result, the dispersion relation of the SO perturbed 1D bands are strongly distorted compared to the original ones, see [24] and Fig.2. Eigen wave functions do not correspond to uniformly polarized spin states but to more complex spatially non uniform spin textures. These band distortions also yield different velocity modulus along the x axis for the pairs of states crossing the Fermi energy, this velocity shift is maximum when the chemical potential sits close to the bottom of the upper energy spin-split subbands [4, 7] as in Fig. 1.

The Andreev states split into 2 families corresponding to different spin states which also have different velocities v^+ and v^- along the x axis (see Fig.1). As shown in Fig.2(right) the eigen-energies of these states cross at 0 andπ as expected from time reversal symmetry. In the long junction limit, the phase dependence of Andreev states is determined by the Fermi velocity, their spin degeneracy is therefore lifted for phase values different from 0 and π by a quantity $\delta\epsilon_S$ of the order of $\hbar\pi(|v^+|-|v^-|/L)$ which can be of the order of $0.5\delta\epsilon$ where $\delta\epsilon$ is the average level spacing. This mixing between transverse channels in a quantum wire induced by SO interaction was already discussed in a different context by Yokohama et al. in short junctions [9] as the condition to observe an anomalous Josephson current at $\phi = 0$ in the presence of a Zeeman field along the y axis (the so called ϕ_0 junction behavior predicted by Buzdin [8] and only recently observed [12, 22]. It is interesting that the conditions for observing spin split Andreev states in zero Zeeman field and a finite Josephson current at zero phase in the presence of an in plane Zeeman field (ϕ_0 junction behavior),[9] are identical in long junctions, see also appendix.

When increasing the number of channels and disorder, one enters the diffusive regime. We still find a sizable splitting of Andreev levels which is of the order of the level spacing. Whereas in the ballistic regime SO interactions tend to reduce the phase dependence of the Andreev levels, we observe instead an increase of this phase dependence in the diffusive regime with a more pronounced harmonics content of the phase dependence of the eigen-energies. This splitting of Andreev levels is therefore a very robust phenomenon in long SNS junctions with SO interaction and shows that the supercurrent in long SNS junctions is in general associated to a spin current of the order of $\mu_B(|v^+| - |v^-|)/L$.

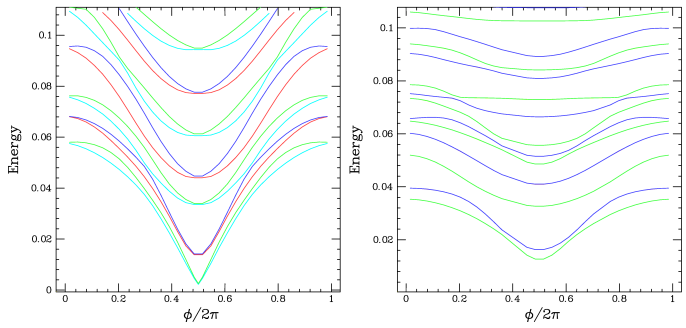

FIG. 3: Phase dependent spectrum of Andreev levels, for a diffusive wire with $N_x^N = 50 \times 20$ normal sites and on site disorder of amplitude $W/t = 1$ corresponding to $L/l_e \simeq 2.5$. (The number of S sites with $\Delta = t/4$ is $N^S = 30 \times 20$), with Rashba spin-orbit interaction $\lambda = 3\Delta$ (left) and without (right). Note the lifting of spin-degeneracy as well as larger and sharper phase dependence of Andreev levels in the presence of spin-orbit interactions.

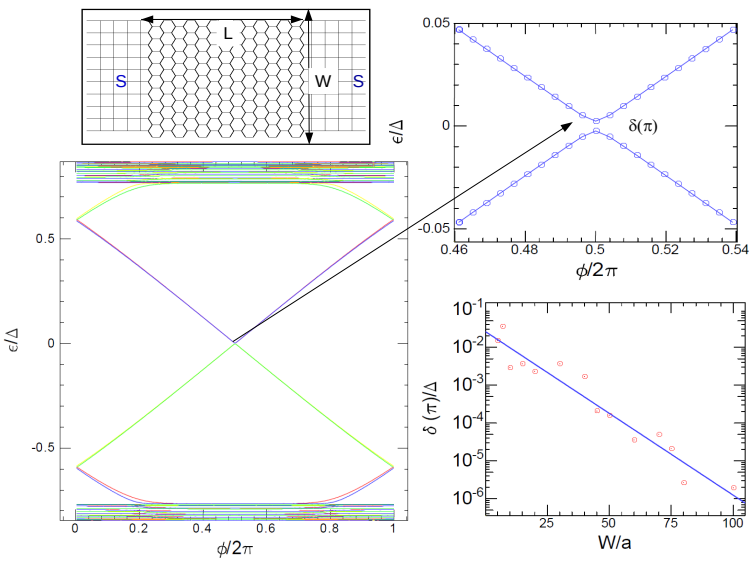

FIG. 4: A ribbon with hexagonal lattice (dimensions $L = N_x a$ and $W = N_y a$) with second neighbour spin-orbit interactions is connected to superconducting electrodes (square lattice). The Andreev sepctrum is shown for $N_x = N_y = 20$ with on site disorder $W = t$, corresponding to the diffusive regime in the absence of SO interaction. The amplitude of SO interaction is equal to the superconducting gap. Fermi energy is chosen to be $\epsilon_F = -0.33t$ and sits in the spin-orbit gap. The spectrum consists in two chiral Andreev levels corresponding to the two edges of the sample (short junction limit). These states exhibit a linear phase dependence and cross each other at zero energy at phase π. Inset: residual gap at $\phi = \pi$ as function of the sample width W.

Hexagonal lattice and quantum spin Hall edge states

We now discuss the Andreev spectrum of graphene-like ribbons with $N^N = N_x \times N_y$ sites on an hexagonal lattice oriented along the armchair direction, in contact with two superconducting electrodes ($N^S = N_x^S \times N_y$ sites) on a square lattice (inset of Fig.4). Following the model of Kane and Mele [1] the spin-orbit interaction is now implemented on the next nearest neighbors (in contrast with eq.3) according to:

$$H_{SO} = \sum_{s,s'=+,-} \sum_{i,j} +i\lambda_{ij}\sigma_{\mathbf{z}}|i,s><j,s'| + C.C. \quad (4)$$

with$\lambda_{ij} = -\lambda_{ji}$. This model is equivalent at very low energy to the implementation of an 'intrinsic' spin-orbit interaction which couples the real spin to the pseudo spin and is opposite in sign for the 2 valleys of the Dirac spectrum. It leads to the opening of opposite spin-orbit gaps at the Dirac points of the 2 valleys and the formation of 2 counter- propagating spin-polarized edge states characteristic of a 2D topological insulator. When the Fermi level sits in this spin-orbit gap, the Andreev spectrum is identical to the spectrum of a single channel ballistic wire with 2 degenerate states crossing at zero energy for $\phi = \pi$. They correspond to the two helical edge states on the 2 sides of the wire not connected to superconducting electrodes (see Fig. 4). There is no degeneracy breaking if there si no Rashba contribution. As expected, this spectrum shown in Fig.4 is very robust against disorder or barriers at the NS interface, which strongly modify the Andreev spectrum in the absence of SO interaction. Is does not depend on the transverse number of sites when the width of the sample is much greater than the superconducting coherence length. The small residual avoided crossing observed is due to the small coupling between the 2 edge states due to the finite width of the sample. We find that this residual gap atπ, $\delta(\pi)$ decreases exponentially with the distance between the edges (i.e. the width of the sample) with a characteristic length given by the superconducting coherence length $\xi_S \simeq 10a$.

JOSEPHSON CURRENT

At zero temperature, the Josephson current $I_J(\phi) = (2\pi/\phi_0)\partial E_J/\partial\phi$ is the derivative of the Josephson Energy E_J which is the sum of the phase dependent energy levels below the Fermi energy. We first discuss the non topological case corresponding to the square lattice with Rashba SO interaction whose Andreev spectrum are shown in Fig.2 and 3 We have seen in the previous section that the presence of spin-orbit interaction strongly modifies the spectrum by lifting the spin degeneracy, leading to crossings at phases multiple of π . This results in even phase dependent contributions to the single level currents, which are non zero at 0 and π and opposite from one another for reversed spin states, see Fig.5. A small Zeeman field perpendicular to the plane of the wire

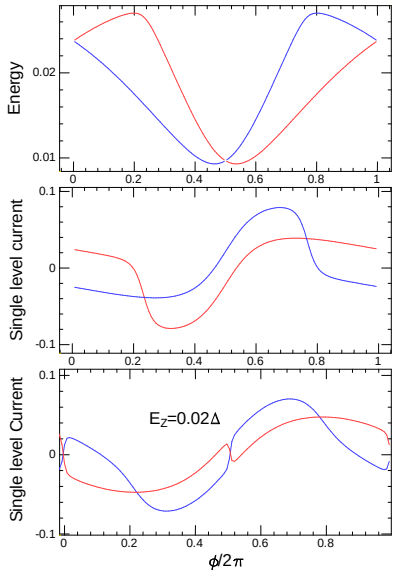

FIG. 5: Top panel: phase dependence of the 2 first levels in the Andreev excitation spectrum of a square lattice tight-binding wire, with Rahshba SO interaction, parameters are $N_x = 130$, $N_y = 4$, $W = 3\Delta$, $\lambda = 2\Delta$. These 2 levels correspond to opposite spin states and cross each other at 0 and π. Middle panel: currents carried by these levels, one can clearly identify a component which is an even function of phase. Bottom same quantity in the presence of a small Zeeman field perpendicular to the wire $E_Z = 0.02$ (in Δ units). Avoided crossings at 0 andπ lead to discontinuities in the single level currents which become odd functions of phase.

lifts degeneracies and induces avoided crossings at multiples of π. The single level currents become therefore odd functions of phase with discontinuities at 0 anπ, see Fig.5. The phase dependence of the total Josephson current is however not affected, due to the compensation between these opposite current contributions of adjacent levels. This is shown in Fig.6 both for ballistic and diffusive wires in the long junction limit whose Andreev spectrum are shown in Fig.1 and Fig.3. One can see that the effect of spin-orbit interactions is opposite in both cases: the ballistic current is decreased whereas an increase of the amplitude of the Josephson current and its harmonics content is observed for the diffusive wire. (This effect may be related to the phenomenon of antilocalisation observed in quantum transport in the presence of spin-orbit interactions [26].) As expected and previously shown in other works [8, 9] the presence of a in plane Zeeman field gives rise to a ϕ_0 behavior accompanied with 0π transitions with discontinuities for certain values of this field, in the current phase relation. This is shown in the appendix.

Different behaviors are found when the normal part of the junction is built from the Kane and Mele topological

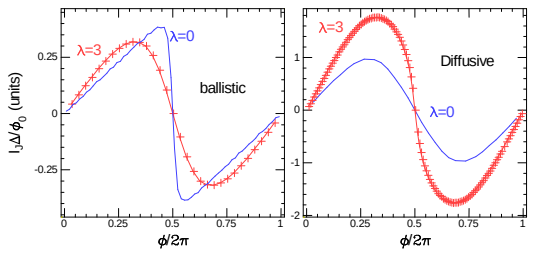

FIG. 6: Effect of spin-orbit interactions on the phase dependent Josephson current for the square lattice with rearrest neighbor Rashba S0 . Left: ballistic wire with $N_y = 2$ (same parameters as Fig.1). Right: diffusive wire in the long junction limit with the same parameters as Fig.3. The amplitude and skewness of the phase dependent Josephson current are decreased in the presence of SO interaction for the ballistic wire whereas they are increased for the diffusive wire.

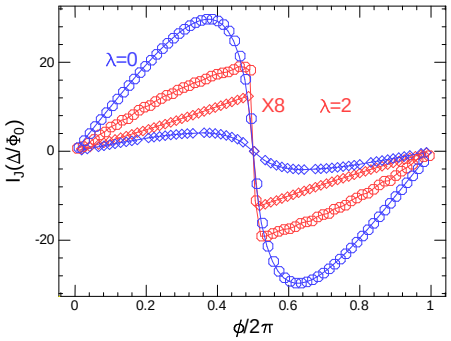

FIG. 7: Effect of S0 interaction on the phase dependent Josephson current: hexagonal lattice without and with ($\lambda = 2\Delta$) next nearest neighbor SO interaction. Parameters are $N_x = 10$ and $N_y = 60$). The Josephson current is strongly modified by spin-orbit interactions and acquires a saw tooth shape with sharp discontinuities at odd multiple values of π which is characteristic of a 1D ballistic SNS junction. The curves with circle points correspond to a small disorder $W/t = 0.02$ and a perfect transmission at the S/N interfaces, whereas diamonds correspond to $W/t = 2$ and a transmission barrier at the S/N interfaces equal to 0.25.

insulator discussed above (hexagonal lattice with next nearest neighbor SO interaction) whose Andreev spectrum is shown in Fig.4. As a result of the formation of topological edge states, the Josephson current is strongly modified by spin orbit interactions and acquires a saw-tooth shape with sharp discontinuities at odd multiple of π which is characteristic of the Josephson current of a single channel ballistic long SNS junction, Fig.7. It is independent of the number of transverse channels and resists to large disorder as well as low transmission interfaces. Measuring this saw tooth current phase relation cannot however be considered as a definite signature of topological edge states. Topological crossings are expected to give rise to a 4π periodicity very difficult to detect experimentally because of unavoidable quasiparticle poisoning

[27].

NON ADIABATIC FINITE FREQUENCY RESPONSE

In this section we show that the finite frequency current susceptibility which is the linear response to an ac phase bias, is much more sensitive to spin orbit interactions than the dc Josephson current discussed above. As previously shown [28, 30, 32, 33] this susceptibility is investigated experimentally in a RF SQUID geometry where a hybrid NS ring is inductively coupled to a microwave cavity generating a small ac flux superimposed to a dc Aharonov Bohm flux . The linear response function relating the ac current to the ac flux bias is described by the complex susceptibility $\chi(\omega) = i\omega Y(\omega)$, ($Y(\omega)$ is the admittance) and can be computed from the eigen-states of the ring using a Kubo formalism [32].

$$\chi(\omega) = \frac{\partial I_J}{\partial \phi} - \sum_n i_n^2 \frac{\partial f_n}{\partial \epsilon_n} \frac{i\omega}{\gamma_D - i\omega} - \sum_{n,m\neq n} |J_{nm}|^2 \frac{f_n - f_m}{\epsilon_n - \epsilon_m} \frac{i\hbar\omega}{i(\epsilon_n - \epsilon_m) - i\hbar\omega + \hbar\gamma_{ND}} \quad (5)$$

J_{nm} is the matrix element of the current operator between the Andreev eigenstates n and m of energies ϵ_n and ϵ_m, f_n is the Fermi Dirac function. The first term is the zero frequency susceptibility of the ring which is the flux derivative of the Josephson current $\chi(0) = \partial I_J/\partial\phi$. The second and third terms only exist at finite frequency and describe the dynamical responses due respectively to the relaxation of the populations χ_D and to the transitions between the levels induced by microwave photons emission or absorption χ_{ND}, the quantities γ_D and γ_{ND} being respectively the diagonal and non diagonal relaxation rates of the system determined by its interaction with its thermodynamic environment. Both χ_D and χ_{ND} give rise to frequency dependent dissipation described by their imaginary components. From now on we focus on χ''_D which yields the largest contribution at low frequency. Note that this contribution is specific to the ring geometry [34] and is ignored in most derivations of the Kubo formula.

$$\chi''_D = -\frac{\omega\tau_{in}}{(1+\omega^2\tau_{in}^2)} \sum_n i_n^2 \frac{\partial f_n}{\partial \epsilon_n} \quad (6)$$

(with $\tau_{in} = \gamma_D^{-1}$). This quantity has a very peculiar phase dependence with a singularity at π in a diffusive wire with a continuous Andreev spectrum, due to the closing of the minigap. It was predicted by Lempitsky in 1983 [29, 31] but only directly measured recently by Dassonneville et al.[30]. When the temperature is large compared to ϵ_n the quantity $\frac{\partial f_n}{\partial \epsilon_n}$ can be approximated by $1/k_BT$ in eq.6. As a result when $T \geq \Delta$, χ''_D is proportional to $S_2 =< \sum_n i_n^2 >$ over the whole spectrum [28, 31]. In the presence of SO interactions Andreev levels are not spin degenerate except at 0 and π leading to level crossings at these points. As a result the single level quantities i_n and i_n^2 are finite at 0 and π as well as their sum S_2. The resulting phase dependence of χ''_D is very different from its characteristic dependence without spin orbit interactions which is zero at multiples of π. Moreover this phase dependence is extremely sensitive to a Zeeman field perpendicular to the wires which couples levels of opposite in-plane spins and opens small gaps at $\phi = n\pi$. These avoided crossings give rise to discontinuities in $i_n(\phi)$ and sharp peaks in i_n^2 and S_2 leading to a phase dependence of χ''_D which exhibits sharp singularities at 0 and π. This extreme sensitivity of χ''_D to a small perpendicular Zeeman field carries the signature of the Rashba spin splitting of Andreev levels as shown in Fig.8comparing the phase dependence of χ''_D with and without Rashba spin orbit interaction. We have so far discussed the phase dependence of χ''_D at temperatures of the order or larger than the superconducting gap. In the low temperature limit, the derivative of the Fermi function in expression 6 selects the very low energy contribution (below k_BT) of the Andreev levels. For a non topological spectrum χ''_D vanishes if the temperature is smaller than the energy gap at π separating electrons and hole states. This sensitivity to the existence of absence of energy levels at zero energy can be exploited to reveal the presence of topological crossings at zero energy as we discuss below.

We move to the case of the Kane and Mele topological insulator in the presence of protected crossings at zero energy We then expect a single peak in $\chi''_D(\phi)$ at π as shown in Fig.9. In practice because of the presence of the 2 edge states on each side of the wire of finite width, there is a very small avoided crossing of the levels at pi leading to a very sharp and narrow dip in χ_D at $\phi = \pi$. This dip observed for $N_y = 20$ fades out when the width of the sample is larger than the superconducting coherence length. The amplitude of this peak diverges at low temperature like 1/T like the derivative of the Fermi function. It is also very sensitive to the application of a perpendicular Zeeman field yielding 2 split peaks symmetrically around $\phi = \pi$. The experimental observation of the dissipation peak at π in the non adiabatic linear response function and its splitting in a small Zeeman field presents strong similarities with the predictions of [35] in the normal state. It should provide a unique signature of the nature of the level crossing at zero energy and constitutes therefore a stringent check of the topological nature of the Andreev spectrum. It is different from the proposals of ref. [36–38] focused on the contribution of the non diagonal elements coupling fundamental to exited states, χ_{ND}, which contribute at higher frequencies (of the order of the Thouless energy for long junctions). These measurements of the ac current response to a small phase bias can be conducted very close to ther-

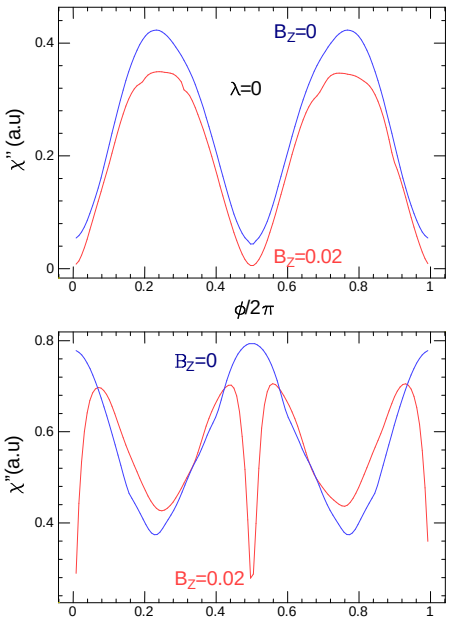

FIG. 8: Phase dependence of χ''_D for the square lattice (non topological regime) at a temperature equal to the superconducting gap as explained in the text, this quantity is close to the average single level current square over the whole spectrum and is nearly π periodic in the absence of spin orbit interactions (upper pannel) nearly insensitive to a small Zeeman field (blue curve $B_Z = 0$, red curve $B_Z = 0.02$). The same quantities are shown the presence of spin orbit interactions $\lambda = 2\Delta$ in the lower panel. Spin splitting and crossings of the energy levels at $\phi = 0$ and π give rise to a very different behavior with broad maxima at 0 and π reflecting levels crossings, and sharp dips in a Zeeman field. Numerical simulations correspond to $N_x = 100$ and $N_y = 4$ with a square lattice. The amplitude of disorder is $W = 3\Delta$.

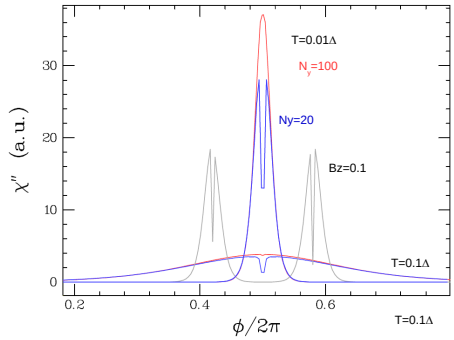

FIG. 9: Phase dependence of χ''_D computed for the hexagonal lattice in the topological regime: SO interaction $\lambda = 2\Delta$, $N_x = 10$, $L = N_y = 60$ (red) and 20 (blue) at temperatures equal to 0.01Δ and 0.1Δ. The peak at π carries the signature of the level crossing in the spectrum and is very sensitive to the presence of a small gap when the width of the sample is of the order of the superconducting coherence length. This gap gives rise to a cancellation of the single level current at π leading to a narrow dip in center of the peak at π. The grey curve is obtained in the presence of a Zeeman field for $N_y = 60$. The effect of the Zeeman field is to split the zero energy level crossing into 2 avoided crossings symmetric around π.

modynamic equilibrium in contrast with the switching current measurements also proposed in [38]. They also allow an independent control of the amplitude and frequency excitation. This is not possible with ac Josephson effect measurements from which it is very difficult to disentangle topological effects from out-of-equilibrium Zener tunneling effects.

We acknowledge R. Aguado, C. Bena, R. Deblock, M. Ferrier, M. Houzet, J. Meyer, H. Pothier, P. Simon and M. Triff for fruitful discussions as well as V. Croquette for great help in making a user friendly interface for the program written by A. Chepelianskii. We have benefited from financial support of the grants MASH ANR-12-BS04-0016 and DIRACFORMAG ANR-14-CE3L-003 of the French agency of research.

[1] C. L. Kane and E. J. Mele, Phys. Rev. Lett. 95, 146802 (2005); 95, 226801 (2005).
[2] Nikolai M. Chtchelkatchev and Yu. V. Nazarov, Phys. Rev. Lett. 90, 226806 (2003).
[3] Beri, Bardarson and C.Beenakker, Phys. Rev. B 77, 045311 (2008).
[4] Andres A. Reynoso, Gonzalo Usaj, C. A. Balseiro, D. Feinberg, and M. Avignon, Phys. Rev. B 86, 214519 (2012).
[5] L. Fu and C. L. Kane, Phys. Rev. Lett., 100, 096407, (2008).
[6] D. Sau, R. M. Lutchyn, S. Tewari, S. Das Sarma, Phys. Rev. Lett. **104**, 040502 (2010), M.Cheng and R. M. Lutchyn Phys. Rev. B**86**, 134522 (2012).
[7] I. V. Krive, L. Y. Gorelik, R. I. Shekhter, and M. Jonson, Low Temperature Physics, 30 398, (2004).
[8] A. Buzdin, Phys. Rev. Lett., 101,107005, (2008).
[9] T. Yokoyama, M. Eto, and Y. V. Nazarov, Phys. Rev. B,90, 195407 (2014).
[10] Konstantin N. Nesterov, Manuel Houzet, and Julia S. Meyer, Phys. Rev. B 93, 174502 (2016).
[11] S. Murakami Phys. Rev. Lett., 97, 236805 (2006).
[12] D. B. Szombati, S. Nadj-Perge, D. Car, S. R. Plissard, E. P. A. M. Bakkers and L. P. Kouwenhoven, Nature Physics 12, 568 (2016).
[13] V. Mourik, K. Zuo, S. M. Frolov, S. R. Plissard, E. P. a. M. Bakkers, and L. P. Kouwenhoven, Science, 336, 6084 (2012).
[14] M. T. Deng, C. L. Yu, G. Y. Huang, M. Larsson, P. Caroff, and H. Q. Xu, NanoLett. 12 6114 (2012).
[15] A. D. K. Finck, D. J. Van Harlingen, P. K. Mohseni, K.

Jung, and X. Li, Phys. Rev. Lett., 110, 126406 (2013).
[16] H. Zhang, Onder Gul, S. Conesa-Boj, K. Zuo, V. Mourik, F. K. de Vries, J. van Veen, D. J. van Woerkom, M. P. Nowak, M.
Wimmer, D. Car, S. Plissard, E. P. A. M. Bakkers, M. Quintero-Pérez, S. Goswami, K. Watanabe, T. Taniguchi, and L. P. Kouwenhoven, arXiv:1603.04069 [cond-mat] (2016).
[17] S. M. Albrecht, A. P. Higginbotham, M. Madsen, F. Kuemmeth, T. S. Jespersen, J. Nygard, P. Krogstrup and C. M. Marcus, Nature 531 206 (2016).
[18] S. Hart, H. Ren, T. Wagner, P. Leubner, M. Malbauer, C. Brune, H. Buhmann, L. W. Molenkamp, and A. Yacoby, Nat.Phys.10 643, (2014).
[19] V. S. Pribiag, A. J. A. Beukman, F. Qu, M. C. Cassidy, C. Charpentier, W. Wegscheider, and L. P. Kouwenhoven, Nat Nano, vol. 10, 593 (2015).
[20] Wiedenmann, E. Bocquillon, R. S. Deacon, S. Hartinger, O. Herrmann, T. M. Klapwijk, L. Maier, C. Ames, C. Brüne, C.
Gould, A. Oiwa, K. Ishibashi, S. Tarucha, H. Bühmann, and L. W. Molenkamp, Nat Commun, 7, 10303, (2016).
[21] Chuan Li, A. Kasumov, Anil Murani, Shamashis Sengupta, F. Fortuna, K. Napolskii, D. Koshkodaev, G. Tsirlina, Y. Kasumov, I. Khodos, R. Deblock, M. Ferrier, S. Guéron, and H. Bouchiat, Phys. Rev. B 90, 245427 (2014).
[22] Anil Murani, Alik Kasumov, Shamashis Sengupta, Yu.A. Kasumov, V.T.Volkov, I.I. Khodos, F. Brisset, Raphaelle Delagrange, Alexei Chepelianskii, Richard Deblock, Helene Bouchiat, and Sophie Guéron, arXiv:1609.04848 (2016).
[23] Bychkov, Y. A. Rasbha, E. I. P. Zh. Eksp. Teor. Fiz. 39, 66 (1984).
[24] M. Governale and U. Zülicke, Spin accumulation in quantum wires with strong Rashba spin-orbit coupling, Phys. Rev. B, 66, 073311 (2002).
[25] G. Montambaux, H. Bouchiat, D. Sigeti, and R. Friesner, Phys. Rev.B 42, 7647 (1990).
[26] Physics Report 107,1 (1984).
[27] Beenakker CWJ, Pikulin DI, Hyart T, Schomerus H, Dahlhaus JP. Phys Rev Lett.110, 1 (2013).
[28] F. Chiodi, M. Ferrier, K. Tikhonov, P. Virtanen, T. Heikkilá, M. Feigelman, S. Guéron, and H.Bouchiat, Sci. Rep. 1, 3 (2011).
[29] Lempitsky, S.V. Sov. Phys. JETP 58, 624 (1983).
[30] B. Dassonneville, M. Ferrier, S. Guéron, and H. Bouchiat, Phys. Rev. Lett., 110, 17001, (2013).
[31] P. Virtanen, F. S. Bergeret, J. C. Cuevas, and T. T. Heikkilá, Phys. Rev. B 83, 144514 (2011).
[32] M. Ferrier, B. Dassonneville, S. Guéron, and H. Bouchiat Phys. Rev. B 88, 174505 (2013).
[33] K. S. Tikhonov and M. V. Feigelman Phys. Rev. B91, 054519 (2015).
[34] Trivedi, N. and Browne, D.A. Mesoscopic ring in a magnetic field: Reactive and dissipative response. Phys. Rev. B 38, 9581 (1988).
[35] Doru Sticlet and Jérome Cayssol Phys. Rev. B 90, 201303(R) (2014).
[36] Jukka I. Värynen, Gianluca Rastelli, Wolfgang Belzig, and Leonid I. Glazman, Phys. Rev. B 92, 134508 (2015).
[37] O. Dmytruk, M. Trif, P. Simon, Phys. Rev. B 92, 245432 (2015); Phys. Rev. B 94, 115423 (2016).
[38] Yang Peng, Falko Pientka, Erez Berg, Yuval Oreg, Felix von Oppen, Phys. Rev. B 94, 085409 (2016).

Appendix: Anomalous Josephson current

We show below the $\phi_0$junction behavior in a 2 channel wire with Rashba SO coupling.

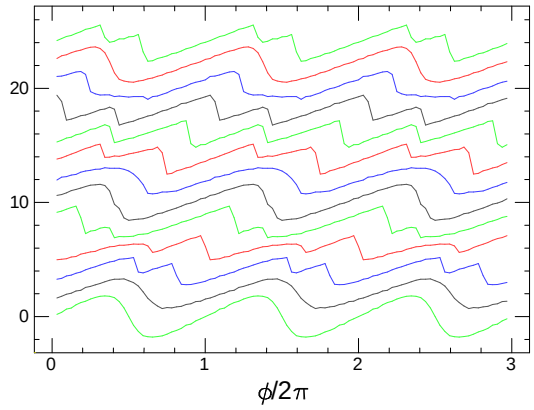

FIG. 10: The phase dependent Josephson current is shown for different values of in plane Zeeman field B_Z perpendicular to the wire going from 0 to 0.12 from bottom to top (in Δ units). One observes a continuous phase shift of the Josephson relations together with abrupt discontinuities for certain values of B_Z. he Fermi energy is taken at 1/4 of the tight binding lower 1D band.(Other parameters are $N_x = 80$, $W = 0.1\Delta$, $\lambda = 3\Delta$)